applied sciences

MDPI

Article

Prediction of Buildings' Settlement Induced by Metro Station Deep Foundation Pit Construction

Shuting Xu and Jinming Xu *

Department of Civil Engineering, Shanghai University, Shanghai 200444, China
* Correspondence: xjming211@163.com

Abstract: The construction of deep foundation pits in subway stations can affect the settlement of existing buildings adjacent to the pits to varying degrees. In this paper, the Long Short-Term Memory neural network prediction model of building settlement caused by deep foundation pit construction was established using the monitoring data of building settlement around a deep foundation pit project in a metro station in Shanghai, and appropriate hyperparameters including batch size and training set ratio were determined. The accuracy of settlement prediction for single-point and multi-point monitoring of buildings was analyzed. Meanwhile, the effects of construction parameters, engineering geological parameters, and spatial parameters on the accuracy of building settlement prediction were investigated. The results show that the batch size and training set proportion can be taken as 16 and 60%, respectively, when using the Long Short-Term Memory neural network prediction model. The proposed Long Short-Term Memory network model can stably predict the settlement of buildings adjacent to deep foundation pits. The accuracy of settlement prediction at a single point of a building (80%) is lower than the accuracy of coordinated prediction at multiple points (88%). More accurate settlement prediction is achieved with the total reverse construction method. The more detailed the consideration of working conditions, geological parameters, and spatial parameters, the better. The evaluation metrics of the prediction model, RMSE, MAE, and R^2, were 0.57 mm, 0.65 mm, and 0.91, respectively. The results of this paper have some practical reference value for analyzing the settlement of buildings caused by foundation pit works.

Keywords: Long Short-Term Memory neural network; construction conditions; settlement prediction; geotechnical parameters; spatial parameters

check for updates

Citation: Xu, S.; Xu, J. Prediction of Buildings' Settlement Induced by Metro Station Deep Foundation Pit Construction. *Appl. Sci.* **2024**, *14*, 2143. https://doi.org/10.3390/app14052143

Academic Editor: Giuseppe Lacidogna

Received: 5 February 2024
Revised: 19 March 2024
Accepted: 22 March 2024
Published: 24 March 2024

1. Introduction

With the rapid advancement of urbanization, infrastructure projects have maintained a high scale. However, due to the existence of a large number of existing buildings surrounding many pits, excessive soil displacement and ground settlement generated during the construction of deep foundation pits will drive the deformation of adjacent buildings, even cause damage to buildings by tilting [1–4]. When the pit is excavated to the design elevation, even with the presence of supporting reinforcement, it often leads to emergency work conditions in neighboring buildings. Settlement of existing buildings in the vicinity of subway station pits during construction may be caused by a variety of influencing factors, such as complex geological and topographical conditions [5]. Therefore, it is necessary to study the settlement prediction methods and influencing factors of neighboring buildings during excavation of deep foundation pit works.

For the settlement deformation of buildings induced by foundation pit construction, scholars have obtained many research works using measured analysis and numerical simulation [6,7]. Based on the field measurement data, it was found that the building settlement basically occurred after the pit excavation and footing completion, and the maximum lateral displacement of the building was basically consistent with the results of the pit excavation in this environment [8]. In general, settlement of existing buildings caused by pit excavation is mainly related to the foundation type and the distance between the building and the pit [9]. Based on the numerical simulation methods, the numerical model of vertical inhomogeneous settlement of existing buildings during pit excavation was established based on PLAXIS software with 2D model and a two-dimensional model considering the plane strain–stress state, and it was found that pit excavation has a significant effect on the stability of the buildings, which provides a more reliable prediction of the building settlement [10,11]. However, the analysis of field-measured data is relatively homogeneous, and numerical analysis has been criticized for its accuracy and validity due to the fact that creating and validating finite element models is very time-consuming and sensitive to boundary conditions [12].

Building settlement monitoring data belong to time-series data, the traditional prediction model is complicated, the model parameters are difficult to determine, and the dynamic prediction of settlement is not effective. Existing studies usually take the surface settlement as the settlement of the surrounding buildings. Simplified equations for predicting settlement were proposed by simplified assessment of building damage caused by pit excavation [13]. The results of predicting building settlement using a non-isometric grey model are better than other grey models, with a 30% improvement in fitting results over the original model [14,15]. Deep learning can process a large amount of time-series data quickly and has been used by many scholars in recent years for the settlement calendar change problem. The use of neural networks to predict the settlement of a single foothold on soft soil reinforced with rigid inclusions revealed that the important input parameters in the network are cohesion, angle of internal friction, and Young's modulus [16]. The settlement of shallow foundations on gypsum soils was predicted using artificial neural networks, and convergence of predicted values with true values was found [17]. Learning and training samples of the back-propagation neural network were established by numerical software, and then, inverse analyses of the roadbed response coefficient K were carried out using the neural network [18]. A regression model was used to predict tunnel-induced ground settlement [19]. Deep learning can process a large amount of time-series data quickly and has been used by many scholars in recent years to deal with the problem of sedimentation ephemeral variation. By establishing a combined prediction model based on the S-shaped growth curve, it was found that the model not only reflected the change process of settlement but also predicted the surface settlement more accurately [20]. By inputting geological conditions, construction parameters, construction sequence, grouting volume, and grouting time, the ground settlement caused by shield tunnel construction was predicted by using an optimized neural network based on a differential algorithm [21]. The ground settlement caused by tunnel excavation was predicted by analyzing the relationship between ground settlement and shield tunneling parameters, and the analysis results were used as inputs to the BP neural network training model [22]. Based on the measured data, the surface settlement caused by tunnel excavation in karst areas was predicted using an extended one-dimensional convolutional neural network model [23]. In order to provide the reader with an intuitive view of the existing research, the authors have classified the relevant literature in Table 1.

Table 1. Classification of available research methods.

Classification	Specific Methods
Traditional methods	Numerical modeling Theoretical equations
Empirical methods	Grey models Neural networks Regression models Curve-fitting methods

For long time-series data, the traditional back-propagation neural network model is simple in structure and unable to capture the changing features of the series, and the recurrent neural network suffers from gradient vanishing; however, the long- and short-term memory neural network better ameliorates these problems by setting up the control unit. The LSTM (Long Short-Term Memory) neural network was widely used for various tasks, such as speech recognition, sound modeling, and correlation analysis [24–27]. Of course, many scholars in different fields have utilized this neural network to predict long time-series data. For example, in the field of civil engineering, some scholars predicted rock shear strength parameters (cohesion and internal friction angle) by constructing a long short-term memory neural network [28]. Some scholars used bidirectional stacked long short-term memory neural networks to predict soil movement [29]. Some scholars predicted hydrological data and drilling logs based on improved LSTM models [30,31]. In the field of economics, some scholars used LSTM neural networks to predict stock returns and stock price movements [32,33]. Some scholars have quantitative stock selection strategies based on CNN (convolutional neural networks)–LSTM neural networks [34].

Currently, most of these research studies use neural networks to map the relationship between static parameters such as soil properties and surface settlement [35], ignoring the fact that deep foundation construction causes surface settlement as well as excessive building settlement. Moreover, building settlement may be affected by time-dependent dynamic factors such as construction conditions. For a subway station deep foundation pit project, the construction conditions are complex, the construction period is long, and the time for different construction conditions is different. For example, there is a big difference between the time period of enclosure construction and reinforcement construction, which often has different impacts on the settlement of the building. At the same time, the model prediction accuracy needs to be analyzed. Both static and dynamic parameters affect the accuracy of building settlement prediction models. The hyperparameters of the model, such as batch size, need to be parameter-optimized [36].

The paper proposes a data-driven model for predicting the settlement of five buildings around a foundation pit. There have been a number of studies using machine learning. Machine learning methods are used to develop empirical susceptibility prediction models [37,38]. Calibrated code-based seismic vulnerability indices were predicted by developing several regression and classification models on a dataset including nearly 300 buildings [39]. Different machine learning methods were used to predict the maximum surface settlement caused by tunnel excavation [40]. In addition, machine learning has been widely applied to other tunnel-related predictions [41,42].

Therefore, this paper intends to take a deep foundation pit project of a metro station in Shanghai as the research background, and based on the LSTM artificial neural network, to artificially determine the reference values of the main hyperparameters of the model (batch size, training set ratio), and then to establish the prediction model of the settlement of neighboring buildings in the construction of deep foundation pits. We then compare the accuracy of single-point settlement prediction and cooperative prediction of multi-point settlement of buildings, study the influence of construction parameters (construction method, construction conditions), engineering geological parameters (unit weight, cohesion, internal friction angle, Poisson's ratio, and void's ratio), and spatial parameters (vertical and horizontal) on the accuracy of the settlement prediction model of the building, and validate the LSTM neural network through the actual monitoring data, the network prediction results, and the evaluation indexes. The accuracy of the building settlement prediction model is verified by actual monitoring data, network prediction results, and evaluation indexes. The research results can provide a certain reference for the safe construction and normal operation of the foundation pit project.

2. Engineering Overview

2.1. Layout of Building Monitoring Points

Shanghai Rail Transit Line 15 is a north–south radial line in the western part of Shanghai, passing through five administrative districts including Minhang District, Xuhui District, Changning District, Putuo District, and Baoshan District. Guilin Road Station is located in Xuhui District and is surrounded by complex buildings and pipelines. The station is an underground three-story island-type platform station, station center mileage SK20+511.173, the total length of the station body is 486.37 m, the net width of the station center is 22.84 m, and the width of the effective platform is 14 m. The planned ground elevation is +4.06 m, the soil overlay at the center of the platform is about 4.31 m, and the elevation of the rail surface in the center of the station is −19.42 m. the main body of the station is a concrete box-type structure cast in situ, of which axes 1~48 are a double-column three-span structure, axes 48~56 are a column-free single-span structure, and axes 56–58 are a single-column double-span structure. The main body of the station is a cast-in-place concrete box structure, of which 1~48 are a double-column three-span structure, axes 48~56 are a column-free single-span structure, and axes 56–58 are a single-column double-span structure. The subway station pit is a long pit with an average depth of about 25.8 m. It is divided into six zones from A to F. Among them, A, C, and E are constructed by the open-cut method, and B, D, and F are constructed by the total reverse method. There are three main buildings around Area A (denoted by I, J, K) and two main buildings around Area F (denoted by P, Q). The arrangement of monitoring points of each building is shown in Figure 1.

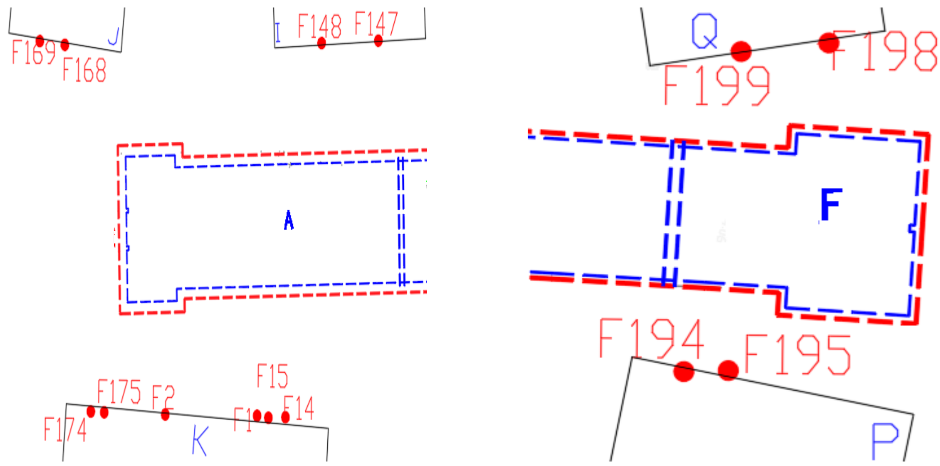

(**a**) (**b**)

Figure 1. Layout of buildings' measuring points. (**a**) Building monitoring points in Area A. (**b**) Building monitoring points in Area F.

2.2. Construction Parameters

The pit in Area A was constructed using the open-cut method, and the pit in Area F was constructed using the full reverse method. Among them, working condition 1 is that the soil body is in an equilibrium state of ground stress before the construction starts. Condition 2 is the use of a 65 + 15 m diaphragm wall as the enclosure structure, which not only plays the role of retaining soil but also serves as the reference and load-bearing structure during the construction process. Condition 3 is the use of grouting reinforcement for the foundation pit, which can effectively prevent the foundation pit from collapsing during the excavation process. Rotary piles are used for reinforcement in Zone A, and three-axis mixing piles are used for reinforcement in Zone F. The foundation pit is reinforced by a series of grouting piles in each layer. Condition 4 is to set up support between each layer of soil, two of which are concrete support and the rest are steel support. The support setup for the reverse method is similar to that of the forward method, but at the same time, the roof slab needs to be poured while excavating. Condition 5 is to continue with the next layer of excavation and repeat the process until the bottom of the pit. The different construction methods and working conditions are shown in Table 2.

Table 2. Different construction methods and working conditions.

Working Conditions	Open Cut	Total Reverse
1	Ground Stress Equilibrium	Ground Stress Equilibrium
2	Construction of enclosing structure	Construction of enclosing structure
3	Construction of soil reinforcement at the base of the pit	Construction of soil reinforcement at the base of the pit
4	First layer of earth excavation and shoring	First layer excavation and shoring and pouring of the roof slab
5	Excavation layer by layer	Excavation layer by layer

2.3. Geotechnical Parameters

According to the ground investigation report. The stratum of the site is mainly powdery soil, silty clay, sandy soil, and the soil layers excavated in the foundation pit mainly include ①fill,②$_1$ clay,③$_1$ silty chalky clay,④$_1$ silty clay,⑤$_{1\text{-}1}$ clay,⑤$_{1j}$ clayey chalk with chalky clay, and⑤$_2$ sandy chalk, and the parameters of the soil layers used (including the thickness, unit weight, cohesion, internal friction angle, void's ratio, and Poisson's ratio) are shown in Table 3. The strength parameters of the soil mainly describe the shear strength of the soil, and the commonly used parameters are cohesion and internal friction angle, which describe the bonding forces between soil particles and the shear expansion characteristics of the soil, respectively. The engineering geological profile is shown in Figure 2. The 1–14 black dots in the figure are the sampling positions of geological exploration.

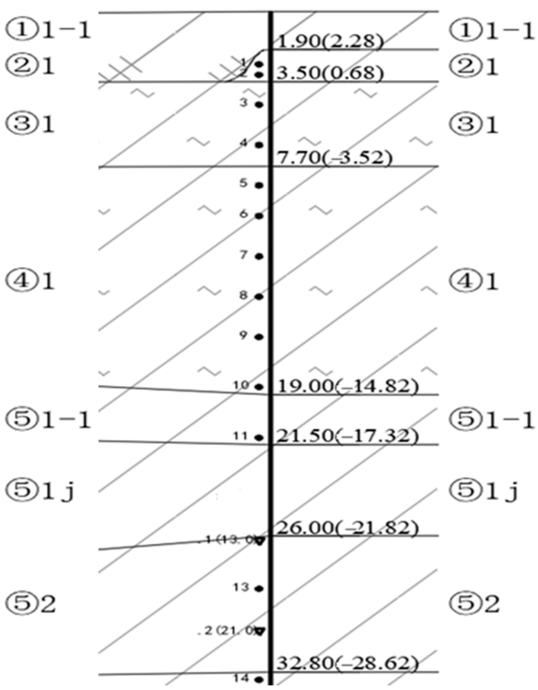

Figure 2. A cross section with geological geotechnical detailing.

Table 3. Soil parameters.

Soil Layer Number	Soil Layer Name	Thickness/m	Unit Weight/kN·m^{-3}	Cohesion/kPa	Internal Friction Angle/°	Void's Ratio	Poisson's Ratio
1	fill	1.9	17.5	8	10	1.06	0.31
2	clay	1.6	17.7	18	17	1.10	0.33
3	silty chalky clay	4.2	17.1	13	12	1.27	0.34
4	silty clay	11.3	16.5	11	13	1.46	0.36
5	clay	3.5	17.2	16	15	1.21	0.34
6	clayey chalk with chalky clay	4.5	17.9	21	12	1.11	0.32
7	sandy chalk	6.8	17.9	31	4	0.99	0.28

2.4. Spatial Parameters

Spatial distribution also plays an important role in the settlement of buildings around the foundation pit. In the process of deep foundation pit construction, the spatial parameters affecting the settlement of buildings are mainly divided into two categories: horizontal spatial parameters and vertical spatial parameters. Vertical spatial parameters include the depth of the soft layer, and the thickness of the soft soil layer where the pit bottom is located (⑤$_2$ sandy silt, thickness of 6 . 8 m) is taken as the vertical spatial input parameter. In addition, the minimum distance between the existing buildings and the station pit is 11.3 m, which means that the frontal distance of all the buildings is less than the excavation depth of the pit *He* (*He* = 25.8 m), and the ground settlement influence zone caused by the soft soil excavation in the Shanghai Metro station may extend to 2–4 *He* behind the pit [43], the horizontal distance between the buildings and the pit also affects the construction process of the pit on the existing buildings' disturbance size. Therefore, in this paper, the horizontal clear distance between the monitoring point of the existing building and the center axis of the foundation pit is selected as the horizontal spatial input parameter of the network.

3. Set Up Buildings' Settlement Prediction Model

3.1. Determination of Datasets for Building Settlement Prediction

3.1.1. Determination of the Initial Dataset

First, the raw data point interval was adjusted from date to days. The continuous settlement monitoring values of each measuring point of the building were selected as the raw data for processing, the data not conforming to the normal distribution were excluded by using the principle of 3σ (the data should meet the range of the mean ± 3 times the standard deviation), and the preliminary dataset was obtained by utilizing the method of linear interpolation to complete the data. For a better understanding by the readers and of the beauty of the picture, part of the initial dataset is shown in Figure 3.

3.1.2. Data Standardization and Anomaly Handling

In order to reduce the influence of the magnitude on the settlement prediction results, the raw monitoring data were standardized, and the standardization formula was:

$$x_i' = \frac{(x_i - \overline{x})}{s} \tag{1}$$

x_i' is the standardized data, x_i is the original monitoring data, $\overline{x}$ is the mean of the original monitoring data, and S is the sample standard deviation of the original monitoring data.

The dataset obtained from the previous section is input into the network for training, the NAN missing values (abnormal data) appearing during the training process need to be deleted from the rows where they are located, and the deleted data rows need to be supplemented to obtain the complete dataset. The final dataset obtained is the settlement monitoring values for 100 days for each of the 14 monitoring points of buildings I, J, K, P, and Q. It is worth mentioning that the dataset used in this paper is relatively small and may not be suitable for overly complex studies.

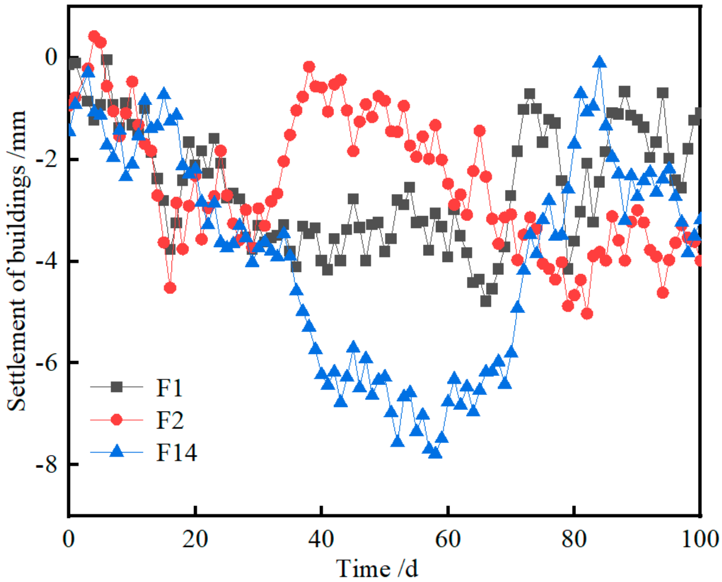

Figure 3. Initial dataset.

3.2. Set Up LSTM Model

3.2.1. LSTM Model

In order to solve the problem of long-term dependency, the Long Short-Term Memory Neural Network was proposed [44]. LSTM is a special network in RNN with a mechanism that can regulate the flow of information, which consists of three kinds of gating, namely input gate, forgetting gate, and output gate, as well as memory cells. The network uses time-series data, the input layer in the network is a known dataset, the hidden layer uses the three gating controls to trade off the data, and the predicted values are obtained from the output layer.

The LSTM model is shown in Figure 4, where X_t and Y_t are the inputs and outputs corresponding to moment t, respectively, σ is the sigmoid activation function, *tanh* is the hyperbolic tangent function, and c_t and h_t are the unit state vectors obtained under the control of the forgetting gate and the final output values obtained under the control of the output gate, respectively. The network flowchart of the building settlement prediction model based on LSTM is shown in Figure 4a. Figure 4b includes the Oblivion gate calculation system, the input gate and the current candidate cell state, the current cell state, the output gate and the final output. The model takes geological parameters, spatial parameters, and building settlement monitoring values as inputs and building settlement predictions as outputs.

In this paper, the settlement prediction model of neighboring buildings for deep foundation pit construction is set up with multiple hidden layers, and the LSTM layer is connected with the dense layer sequentially; the initial learning rate, the number of hidden units, the maximum number of back generation rounds, and the dropout are taken to be 0.007, 100, 80, and 0.2, respectively; and the loss transfer adopts the Adam algorithm.

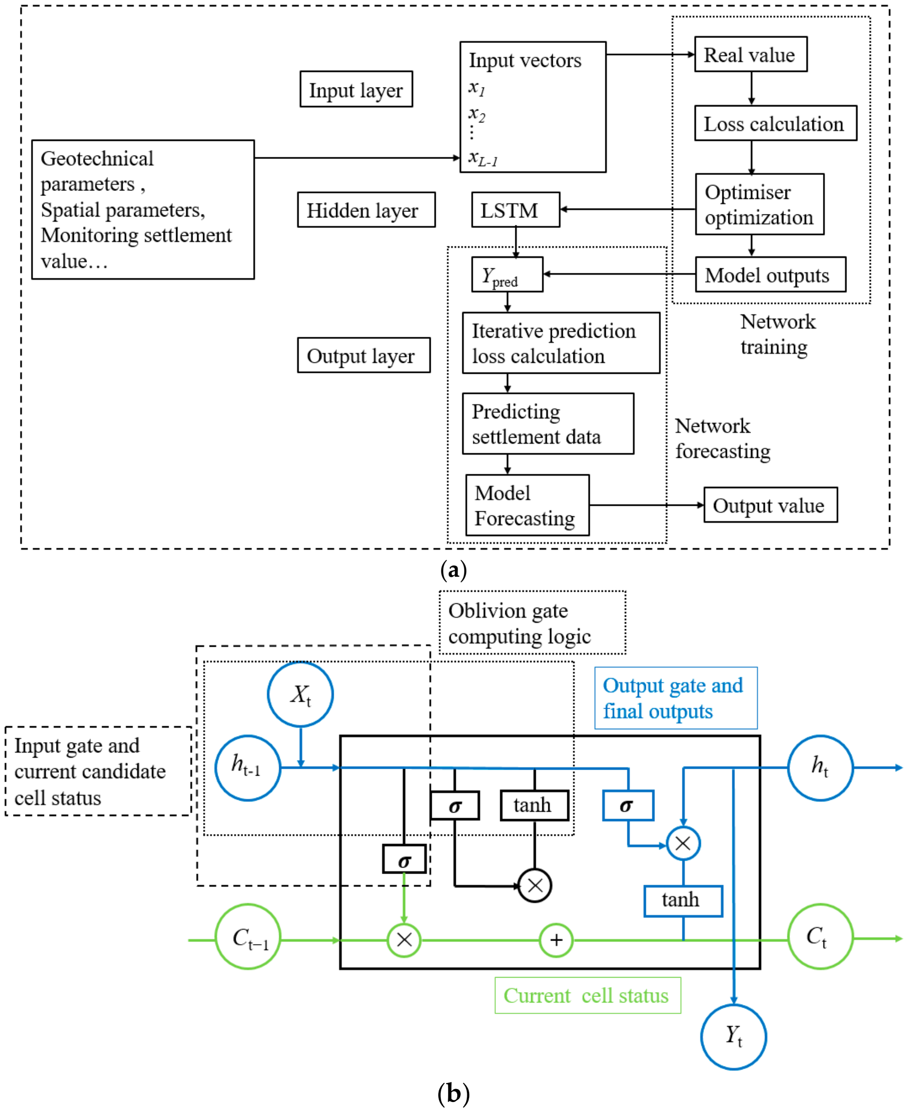

Figure 4. LSTM model. (**a**) Model prediction flowchart. (**b**) LSTM unit structure.

3.2.2. Network Evaluation Metrics

In order to examine the accuracy of the prediction results of the LSTM neural network, four indexes, namely root-mean-square error (RMSE), mean absolute error (MAE), coefficient of determination (R^2), and relative error (maximum error between predicted and monitored values $\times$ 100%, expressed as the letter E), were selected to evaluate the accuracy of the prediction model. Among them, the root-mean-square error can visualize the dispersion between the predicted values and the monitoring data of the network model and is easy to calculate; the mean absolute error can measure the average modal length of the error but does not take the direction into account; and the coefficient of determination can measure the explanatory ability of the model for the dependent variable. The formulas for root-mean-square error, mean absolute error, and coefficient of determination are as follows:

$$\mathrm{RMSE} = \sqrt{\frac{1}{n}\sum_{i=1}^{n}(\hat{y}_i - y_i)^2} \tag{2}$$

$$\mathrm{MAE} = \frac{1}{n}\sum_{i=1}^{n}|\hat{y}_i - y_i| \tag{3}$$

$$R^2 = \frac{\sum_{i=1}^{n} (\hat{y}_i - \overline{y})}{\sum_{i=1}^{n} (y_i - \overline{y})} \tag{4}$$

$$\mathrm{E} = \left| \frac{\hat{y}_i - y_i}{y_i} \right| \times 100\% \tag{5}$$

where $\hat{y}_i$ is the predicted value; $\overline{y}$ is the average value of the monitoring data; y_i is the monitoring data; n is the number of monitoring points; RMSE, MAE, the smaller the predicted value and the monitoring value, the more consistent and accurate the model; R^2 is the overall evaluation of the model's goodness of fit, the value of the range of [0, 1], the closer the R^2 is to 1, the more accurate the model.

3.2.3. Selection of Hyperparameters

Hyperparameter tuning is crucial for LSTM predictive models when the dataset is small [45]. The main hyperparameters that usually need to be tuned before the network starts training are batch size and training set ratio. Among them, the batch size will have an impact on the network accuracy and convergence rate, and in general, 32 was taken as the default value of the batch size [46]. The building settlement dataset in pit engineering is not complex; therefore, the batch size (8, 16, 32, 64, 128) is used for training in this paper. Meanwhile, in traditional model training, 80% of the data are generally used as the training set for model training, and 20% of the data are used as the test set for model effect checking, and the results are often quite different from the actual engineering; therefore, this paper uses the training set ratio (90%, 80%, 70%, 60%, 50%) for training.

The settlement monitoring data of 10 monitoring points (F1, F2, F14, F15, F147, F148, F168, F169, F174, F175) of I–K were input into the model for training, and the model was used to train the monitoring data from each of the 10 measurement sites sequentially. When changing the size of the training batch, the training set ratio was kept constant, and the average of the RMSE was calculated after the training of the 10 measurement points. Similarly, the same is true when changing the training set ratio. The RMSE was used as an evaluation index for the effect of hyperparameters in the model to affect the prediction effect of the settlement [47], and the main hyperparameters of the model were determined by the average of the root-mean-square error of all the measurement points at the time of training (the batch size, the ratio of the training set), and the obtained results can be used as the reference value for the artificial determination of hyperparameters for the prediction of the building settlement by the neural network model.

We input the settlement monitoring data of each measurement point for training, where the basic values of batch size and training set proportion are taken as 32 and 80%, respectively, and the evaluation results under different hyperparameters during the model training are shown in Table 4. In the table, RMSE is the average of the root-mean-square error during the training of 10 measurement points.

Table 4. RMSE of various hyperparameter values during monitoring points training.

Hyperparameters	Value	RMSE (mm)
Batch size	8	0.64
	16	0.59
	32	0.61
	64	0.73
	128	0.71
Training set ratio	90%	0.63
	80%	0.61
	70%	0.67
	60%	0.50
	50%	0.55

The training results show that when the batch size and training set ratio are taken as 16 and 60%, respectively, the average RMSE of the measurement points is the smallest, namely 0.59 and 0.50, respectively. Therefore, when using the LSTM network model for predicting building settlement, the batch size of 16 and the training set ratio of 60% can be used as the reference values for the hyperparameter settings.

3.3. Accuracy Validation of LSTM Neural Network Model

In order to verify the correctness of the constructed LSTM neural network model, the settlement monitoring data from the aforementioned 10 measurement points were sequentially input into the network for training, and the monitored and predicted values of the maximum settlement were obtained as shown in Figure 5.

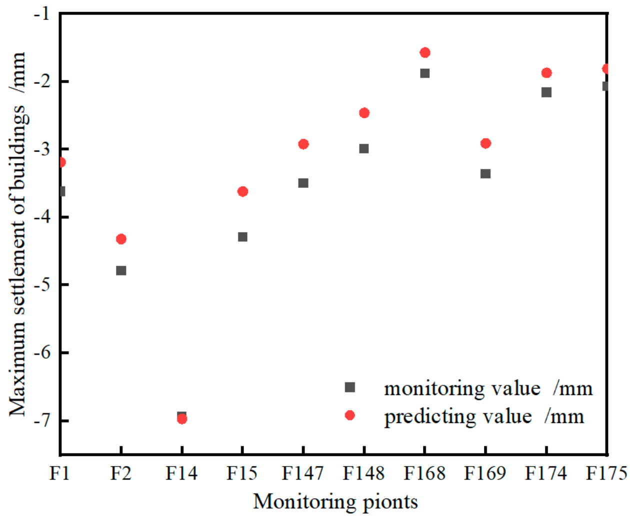

Figure 5. Predicted and monitoring of maximum settlements at measuring points.

As can be seen in Figure 5, the prediction accuracy of the model is more than 82% when predicting the maximum settlement value of a single point of the building, among which, the largest error between the predicted value and the monitoring value occurs at the measurement point F148 (the predicted value is −2.46 mm, the monitoring value is −2.99 mm, and the error of both of them is 17.73%), the evaluation indexes of RMSE, MAE, and R^2 are 0.68, 0.54, and 0.83, respectively, the error of the proposed model is small, and the error of the constructed model is small. Therefore, the buildings adjacent to the foundation pit can use the LSTM model constructed in this paper for settlement prediction.

4. Accuracy Analysis of LSTM Network Models for Predicting Buildings' Settlement

Most of the previous researchers used static parameters to study the accuracy of neural network prediction models; however, dynamic parameters such as construction conditions also have a certain impact on the settlement of the surrounding buildings during the construction of deep foundation pits. Next, this paper will analyze the effects of dynamic parameters (construction conditions) and static parameters (soil properties, spatial parameters) on the accuracy of the prediction model.

4.1. Analysis of the Effect of Construction Parameters on the Accuracy of Model

When the soil body is in the state of equilibrium of geostress, the change in building settlement monitoring value is not obvious. In order to analyze the influence of different construction methods on the accuracy of building settlement prediction under different construction conditions, the settlement monitoring values of the buildings around the pit corresponding to the open excavation method and the full reversal method under conditions 2, 3, and 4 are selected as inputs, and the results obtained by using the LSTM model for prediction are shown in Figures 6 and 7. At the same time, the prediction models used for different conditions are also different, according to the aforementioned model hyperparameter optimization method to determine the parameters of the model for each condition, which are as follows: Condition 2 (batch size of 16, training set ratio of 80%), Condition 3 (batch size of 8, training set ratio of 60%), Condition 4 (batch size of 16, training set ratio of 70%).

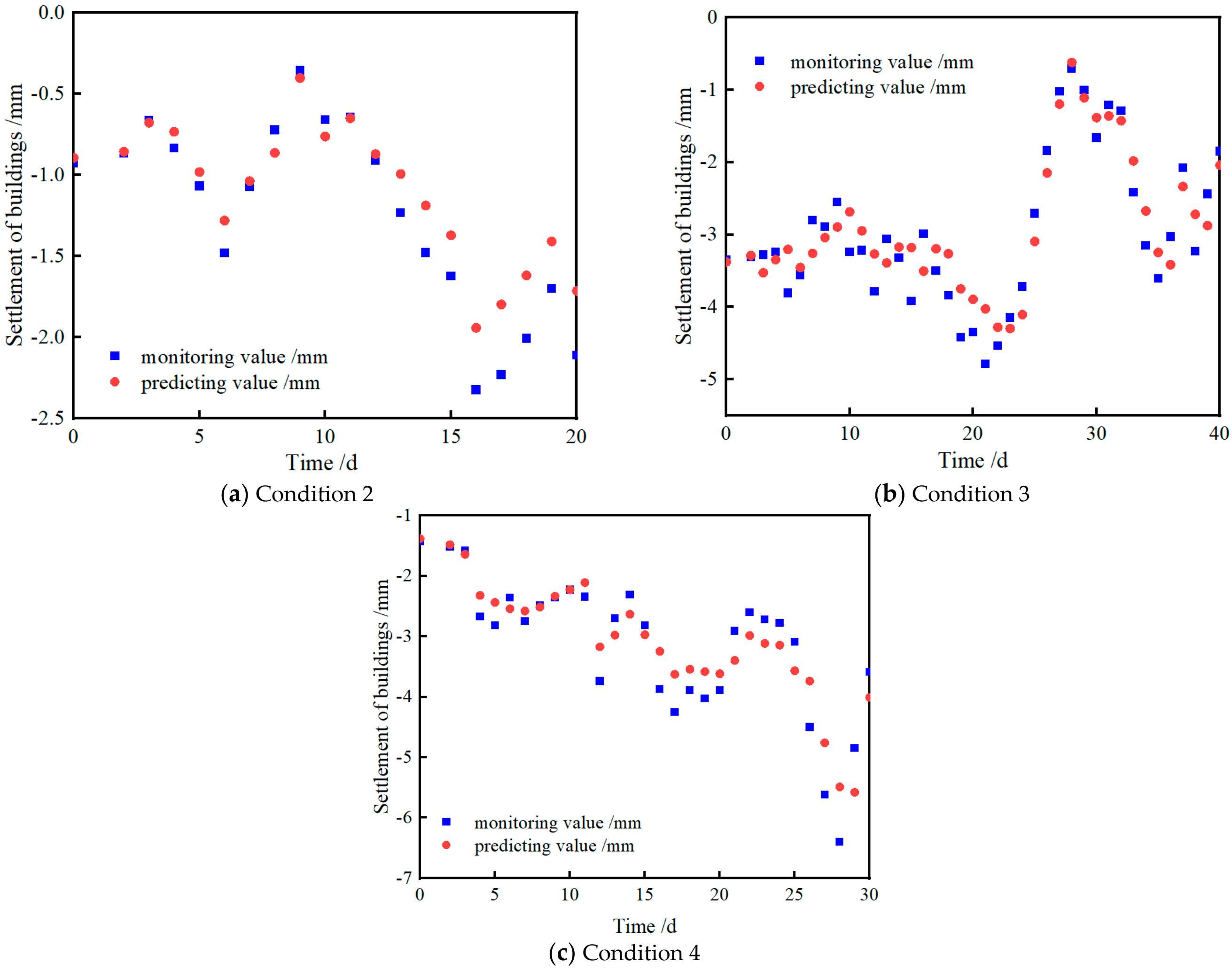

Figure 6. Comparison of settlement monitoring values and predicted values for various conditions of the open-cut method.

As can be seen from Figures 6 and 7, under different working conditions, the predicted building settlement corresponding to the open-cut method and the full reversal method basically coincides with the monitoring values. The average RMSE, MAE, R^2, and relative errors of building settlement prediction under different working conditions are 0.81, 1.01, 0.78, and 18.06%, respectively, while the average RMSE, MAE, R^2, and relative errors of building settlement prediction under full reversal method are 0.78, 0.85, 0.85, and 14.88%, respectively. This indicates that the settlement prediction of the surrounding buildings is more accurate when the pit is constructed using the full reversal method.

Meanwhile, the prediction accuracy of the model varies under different working conditions, and the relative errors of the settlement predictions of the two construction methods are the largest in Working Condition 2 (19.86% and 15.87%, respectively), which may be due to the large disturbance to the soil body caused by grouting reinforcement, which causes the monitoring data to fluctuate greatly. This indicates that different working conditions have a large impact on the accuracy of building settlement prediction, and the working conditions need to be taken into account when using the LSTM model to predict the settlement of buildings around the foundation pit.

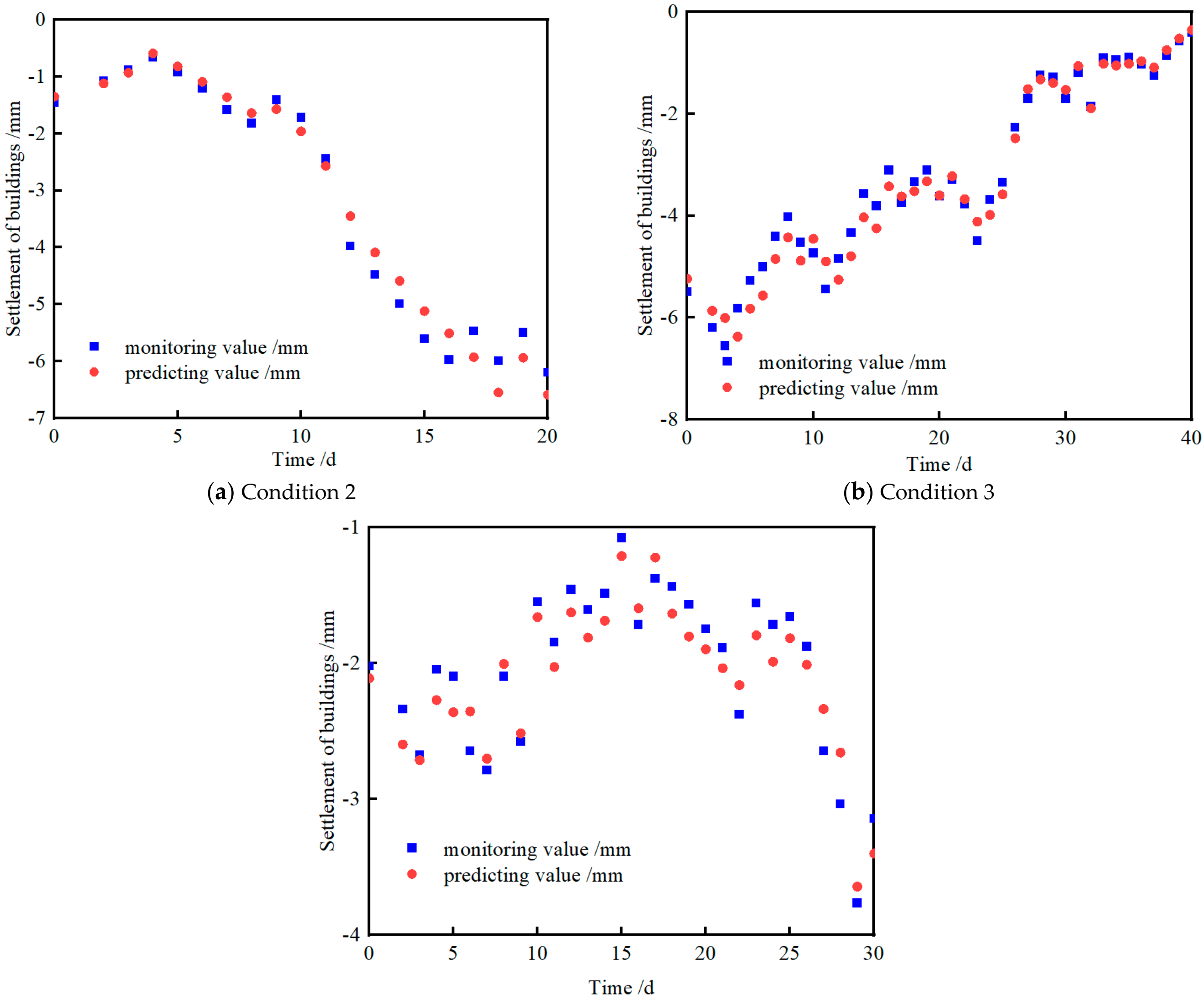

(**a**) Condition 2 (**b**) Condition 3 (**c**) Condition 4

Figure 7. Comparison of settlement monitoring values and predicted values for various conditions of the total reverse method.

4.2. Analysis of the Effect of Engineering Geological Parameters on the Accuracy of Model

The buildings' settlement and deformation in the process of pit construction are closely related to the stratum changes (the stratum parameters in this paper include soil gravity, friction angle, cohesion, Poisson's ratio, and pore ratio); in order to further analyze the influence of the stratum-related parameters on the predicted value of the building settlement, keep the other parameters unchanged, and take the building settlement monitoring values and engineering geological parameters under the three conditions of the total reversal method as input, and the predicted value of the building settlement as output. The prediction results are shown in Figure 8.

As can be seen from Figure 8, the prediction methods with or without considering the effect of stratigraphic changes reflect the same pattern on the predicted values of single-point settlement of buildings. The average relative error of the predictions for the three conditions considering the effect of ground changes is around 8.23%, and the accuracy of the model prediction is improved by 6% compared with the one without considering ground changes.

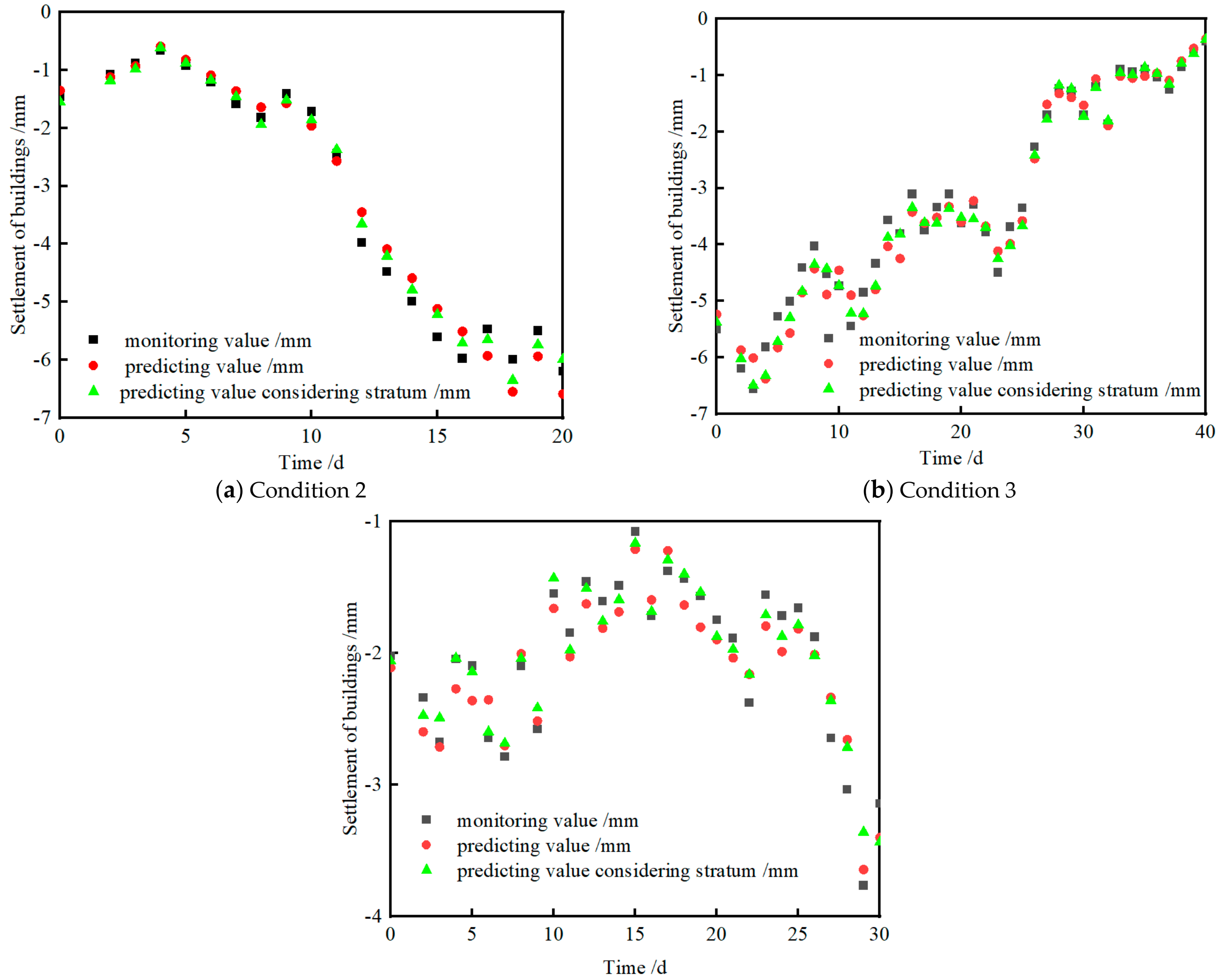

(**a**) Condition 2 (**b**) Condition 3

(**c**) Condition 4

Figure 8. Predicted settlements with and without consideration of soil parameters.

4.3. Analysis of the Effect of Spatial Parameters on the Accuracy of Model

During the construction of a deep foundation pit in a soft soil area, the depth of the soft soil layer and the horizontal distance between the building and the foundation pit have an important influence on the settlement of the neighboring buildings. In order to study the influence of spatial parameters on the accuracy of building settlement prediction, the spatial parameters are now used as inputs together with the settlement monitoring values of the three working conditions of the aforementioned full inversion method considering the stratum changes, and the settlement prediction values are used as outputs. The prediction results are shown in Figure 9.

As can be seen from Figure 9, the trend of the predicted values with or without considering spatial parameters is basically the same as that of the monitored values. The average relative error of the prediction of the three working conditions with space parameters considered is 5.01%, which is 3% higher than the prediction without space parameters. Meanwhile, the average values of the evaluation indexes RMSE, MAE, and R^2 for the three working conditions were 0.57, 0.65, and 0.91, which were improved by 16%, 11%, and 3%, respectively, compared with the evaluation indexes without considering space parameters. This indicates that the LSTM model is more accurate in predicting the settlement of buildings around deep foundation pit construction after considering spatial parameters. The statistical results of each prediction as well as the findings of other scholars are shown in Table 5.

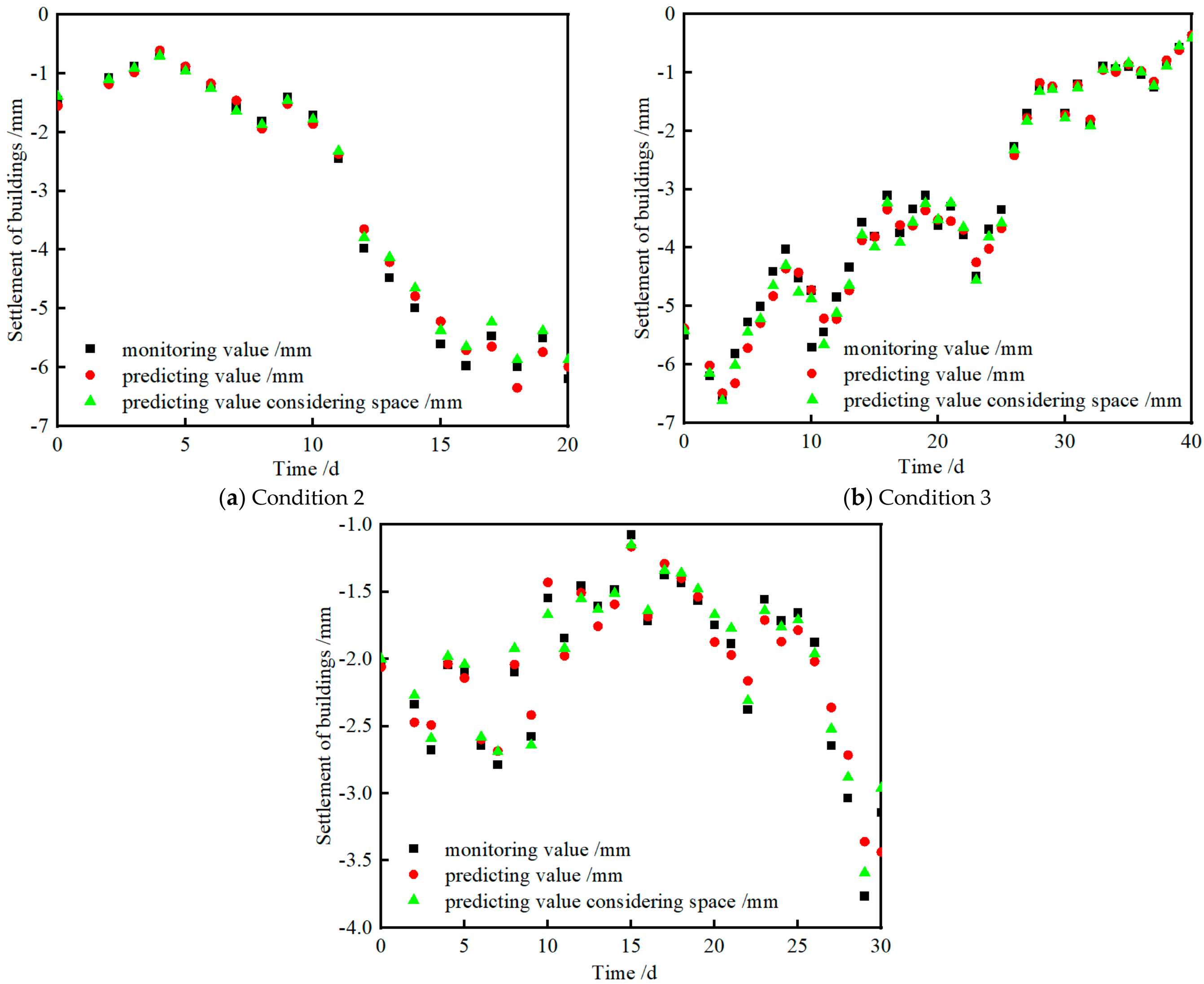

(**a**) Condition 2

(**b**) Condition 3

(**c**) Condition 4

Figure 9. Settlement prediction considering spatial parameters under various working conditions.

Table 5. Adjustment statistics.

Input Parameters	RMSE (mm)	MAE (mm)	R^2
Condition	0.78	0.85	0.85
Geological	0.68	0.73	0.88
Spatial	0.57	0.65	0.91
Shallal	/	0.73	0.70
Ou	/	/	0.95

After considering geological and spatial parameters, the evaluation metrics of the model, MAE and R^2 were 0.65 and 0.91, respectively. Shallal's network evaluation metrics, MAE and R^2, for predicting settlement using Artificial Neural Network (ANN) were 0.73 and 0.70, respectively [17], compared to which the network model prediction accuracy in this study was improved by 10.96% and 30%, respectively. It indicates that the prediction of building settlement using an LSTM neural network is more accurate than using ANN. It is worth mentioning that the R^2 of this study is 0.91, which is not as good a fit compared to Ou's R^2 (0.95) for predicting settlement using simplified equations [13], but there is only a difference of about 4%, which can be further optimized and improved by adjusting the rest of the hyperparameters of the model, etc.

4.4. Analysis of the Effect of Multi-Point Co-Prediction on the Accuracy of Model

Since there are usually multiple buildings around the pit and multiple measurement points are set up for one building, the buildings will also affect each other, thus aggravating the settlement of each building. Therefore, in addition to the static and dynamic parameters mentioned above that affect the accuracy of the prediction model, the joint prediction of different monitoring points will also have an impact on the model prediction accuracy. Now, the settlement monitoring values of monitoring points F147-148 of I, F168-169 of J, and F1 of K are taken as inputs, and the settlement prediction values of monitoring point F1 are taken as outputs, and the proposed LSTM model is used for the joint prediction of settlement at multiple points of the buildings, and the obtained monitoring values and prediction values are shown in Figure 10.

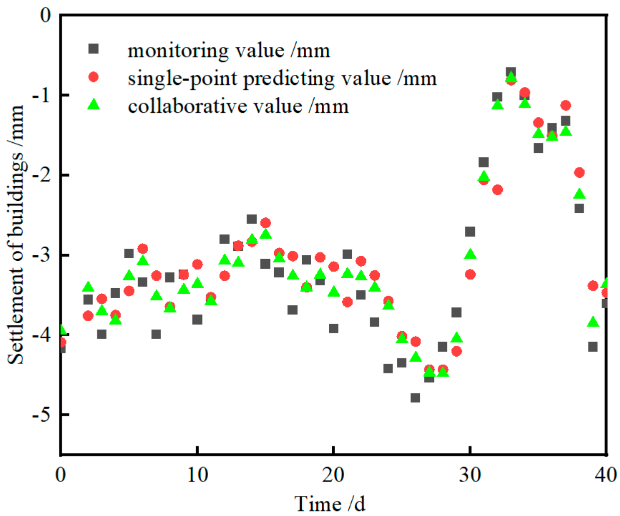

Figure 10. Comparison of single-point predicted and multi-point co-predicted and monitored values.

As can be seen from Figure 10, the change trends of predicted values and monitoring values are basically the same. The maximum relative error between the predicted and monitored values of single-point settlement of the building is 19.96% (the predicted value is −3.59 mm, and the monitored value is −2.99 mm), the prediction accuracy is more than 80%, and the evaluation indexes RMSE, MAE, and R^2 are 0.55, 0.42, and 0.81, respectively. The maximum relative error between the predicted and monitored values of the coordinated prediction of multi-point settlement is 11.79%, the prediction accuracy is more than 88%, and the network evaluation indexes RMSE, MAE, and R^2 are 0.51, 0.37, and 0.89, respectively. The maximum relative error between the predicted value and the monitored value is 11.79%, the accuracy of the prediction is more than 88%, and the network evaluation indexes are 0.51, 0.37, and 0.89 for RMSE, MAE, and R^2, respectively, Compared with the single-point settlement prediction, the accuracy of the multi-point settlement cooperative prediction is increased by 8%, and the evaluation indexes are increased by 7%, 12%, and 10%, respectively, which means that the prediction of the building settlement using the constructed LSTM model is more accurate by taking into consideration the interaction effect of the buildings.

5. Conclusions

Accurate prediction of building settlement near deep foundation pit excavation is a prerequisite for the safe construction of deep foundation pit projects. This paper takes a deep foundation pit project of a metro station in Shanghai as an example, establishes the Long Short-Term Memory (LSTM) settlement prediction model using building settlement monitoring data, and obtains the following conclusions.

(1) Hyperparameters have a key role in the predictive ability of network models. This study explores the effects of batch size and training set ratio on model prediction accuracy and finds that when the batch size and training set ratio are taken as 16 and 60%, respectively, the average values of the network evaluation index RMSE are 0.59 and 0.50, respectively, and the RMSE is smaller, at which time the model established has the best prediction effect.
(2) When the settlement of the buildings around the foundation pit constructed by the full reversal method is selected for prediction, the prediction accuracy of the network model reaches 14.88%, which is about 3% higher than that of the open excavation method, indicating that the prediction value of the long- and short-term memory neural network model is more accurate when the settlement of the buildings around the foundation pit constructed by the full reversal method is used.
(3) The LSTM neural network model established in this paper for predicting the settlement of adjacent buildings caused by deep foundation pit construction has a model accuracy of more than 82%, and the model prediction accuracy is related to the construction parameters (construction conditions), engineering geological parameters (soil gravity, cohesion, friction angle, Poisson's ratio, and pore space ratio), and the more carefully the parameters are considered, the more accurately the model prediction is formulated. The evaluation metrics MAE and R^2 were improved by 10.96% percent and 30%, respectively, compared with the use of an Artificial Neural Network (ANN).
(4) The accuracy of the network model for predicting single-point settlement using multi-point settlement of multiple buildings collaboratively is 88%. However, the accuracy of the network model predicting single-point settlement using single-point settlement is only 80%, which is about 8% lower than the accuracy of the collaborative prediction using multiple monitoring points.
(5) This study investigates the feasibility of using a data-driven model (LSTM neural network) to predict the settlement of surrounding buildings caused by deep foundation pit excavation, and the results of the study can provide a certain basis for the construction of foundation pit projects. The LSTM neural network has the capability of predicting the settlement of surrounding buildings caused by the excavation of a foundation pit with high accuracy. The authors will subsequently try to develop physics-based machine learning to optimize the prediction results of the model.

Author Contributions: Writing—review & editing, S.X.; Funding acquisition, J.X. All authors have read and agreed to the published version of the manuscript.

Funding: This research received no external funding.

Institutional Review Board Statement: Not applicable.

Informed Consent Statement: Not applicable.

Data Availability Statement: The data used to support the findings of this study are included within the article.

Acknowledgments: Grant No. 41472254 from the Natural Science Foundation of China is gratefully acknowledged.

Conflicts of Interest: The authors declare no conflicts of interest.

References

1. Liu, L.; Li, Z.; Cai, G.; Liu, X.; Yan, S. Humidity field characteristics in road embankment constructed with recycled construction wastes. *J. Clean. Prod.* **2020**, *259*, 120977. [CrossRef]
2. Qiao, S.; Tan, J.; Zhang, Y.; Wan, L.; Zhang, M.; Tang, J.; He, Q. Settlement prediction of foundation pit excavation based on the GWO-ELM model considering different states of influence. *Adv. Civ. Eng.* **2021**, *2021*, 8896210.

3. Xu, C.; Yue, D.; Deng, C. Hybrid GA/SIMPLS as alternative regression model in dam deformation analysis. *Eng. App. Art. Int.* **2012**, *25*, 468–475. [CrossRef]
4. Zhou, N.; Vermeer, P.; Lou, R.; Tang, Y.; Jiang, S. Numerical simulation of deep foundation pit dewatering and optimization of controlling land subsidence. *Eng. Geo.* **2010**, *114*, 251–260. [CrossRef]
5. Gero, M.; Gayarre, F.; Fernandez, C.; Llardent, M. Forensic analysis of the failure of the foundations of a tunnel built to channel the course of a river. *Eng. Fail. Anal.* **2013**, *32*, 152–166. [CrossRef]
6. Wang, G.; Chen, W.; Cao, L.; Li, Y.; Liu, S.; Yu, J.; Wang, B. Retaining technology for deep foundation pit excavation adjacent to high-speed railways based on deformation control. *Front. Earth Sci.* **2021**, *9*, 735315. [CrossRef]
7. Wei, H. Influence of foundation pit excavation and precipitation on settlement of surrounding buildings. *Adv. Civ. Eng.* **2021**, *2021*, 6638868. [CrossRef]
8. Lu, C.; Chen, B.; Hu, Y. Environmental impacts of the abnormal settlement of surrounding buildings caused by deep pit excavation in Shanghai. *Ekoloji Derg.* **2018**, *27*, 1337–1343.
9. Tan, Y.; Huang, R.; Kang, Z.; Bin, W. Covered semi-top-down excavation of subway station surrounded by closely spaced buildings in downtown Shanghai: Building response. *J. Perform. Constr. Facil.* **2016**, *30*, 04016040. [CrossRef]
10. Zhang, X.; Yang, J.; Zhang, Y.; Gao, Y. Cause investigation of damages in existing building adjacent to foundation pit in construction. *Eng. Fail. Anal.* **2018**, *83*, 117–124. [CrossRef]
11. Mangushev, R.A.; Osokin, A.I.; Garnyk, L.V. Experience in preserving adjacent buildings during excavation of large foundation pits under conditions of dense development. *Soil Mech. Found.* **2016**, *53*, 291–297. [CrossRef]
12. Zhu, M.; Li, S.; Wei, X.; Wang, P. Prediction and stability assessment of soft foundation settlement of the fishbone-shaped dike near the estuary of the Yangtze river using machine learning methods. *Sustainability* **2021**, *13*, 3744. [CrossRef]
13. Ou, C.; Teng, F.; Li, C. A simplified estimation of excavation-induced ground movements for adjacent building damage potential assessment. *Tunn. Undergr. Space Technol.* **2020**, *106*, 103561. [CrossRef]
14. Zhang, J.; Qin, Y.; Zhang, X.; Che, G.; Sun, X.; Duo, H. Application of non-equidistant GM (1, 1) model based on the fractional-order accumulation in building settlement monitoring. *J. Intell. Fuzzy Syst.* **2022**, *42*, 1559–1573. [CrossRef]
15. Wei, J.; Jiang, H.; Diao, J. Application of non-equidistant gray model based on optimization of background value in settlement prediction. *IOP Conf. Ser. Earth Environ. Sci.* **2021**, *636*, 012004. [CrossRef]
16. Zhang, J.; Dias, D.; An, L.; Li, C. Applying a novel slime mould algorithm-based artificial neural network to predict the settlement of a single footing on a soft soil reinforced by rigid inclusions. *Mech. Adv. Mater Struct.* **2022**, *31*, 422–437. [CrossRef]
17. Shallal, H.; Aljanabi, Q. Prediction of gypseous soil settlement using artificial neural network (ANN). *Diyala J. Eng. Sci.* **2022**, *15*, 89–95. [CrossRef]
18. Miao, J.; Wang, F. Inverse analysis of subgrade reaction coefficient of subway based on computer neural network. *Geotech. Geol. Eng.* **2023**, *41*, 1–13. [CrossRef]
19. Moghaddasi, M.; Noorian-Bidgoli, M. ICA-ANN, ANN and multiple regression models for prediction of surface settlement caused by tunneling. *Tunn. Undergr. Space Technol.* **2018**, *79*, 197–209. [CrossRef]
20. Su, Y.; Wang, X.; Fu, Y.; Zheng, X.; You, G. Research on surface settlement prediction based on the combination prediction model of s-shaped growth curves. *Geo. Eng.* **2018**, *21*, 236–241. [CrossRef]
21. Zhang, K.; Lyu, H.; Shen, S.; Zhou, A.; Yin, Z. Evolutionary hybrid neural network approach to predict shield tunneling induced ground settlements. Tunn. Undergr. *Space Technol.* **2020**, *106*, 103594.
22. Shi, J.; Ortigao, J.; Bai, J. Modular neural networks for predicting settlements during tunneling. *J. Geo. Geo. Eng.* **1998**, *124*, 389–395. [CrossRef]
23. Zhang, N.; Zhou, A.; Pan, Y.; Shen, S. Measurement and prediction of tunneling-induced ground settlement in karst region by using expanding deep learning method. *Measurement* **2021**, *183*, 109700. [CrossRef]
24. Fernández, S.; Graves, A.; Schmidhuber, J. Sequence labelling in structured domains with hierarchical recurrent neural networks. In Proceedings of the 20th International Joint Conference on Artificial Intelligence, Hyderabad, India, 6–12 January 2007; Morgan Kaufmann: San Mateo, CA, USA, 2007.
25. Hsu, W.; Zhang, Y.; Lee, A.; Glass, J. Exploiting depth and highway connections in convolutional recurrent deep neural networks for speech recognition. *Cell* **2016**, *50*, 395–399.
26. Palangi, H.; Deng, L.; Shen, Y.; Gao, J.; He, X.; Chen, J.; Ward, R. Deep sentence embedding using the long short-term memory network: Analysis and application to information retrieval. *IEEE/ACM Trans. Audio Speech Lang. Process.* **2015**, *24*, 694–707. [CrossRef]
27. Mallinar, N.; Rosset, C. Deep canonically correlated LSTMs. *arXiv* **2018**, arXiv:1801.05407.
28. Mahmoodzadeh, A.; Mohammadi, M.; Salim, S.; Ali, H.; Ibrahim, H.; Abdulhamid, S.; Nejati, H.; Rashidi, S. Machine Learning Techniques to Predict Rock Strength Parameters. *Rock Mech. Rock Eng.* **2022**, *55*, 1721–1741. [CrossRef]
29. Kumar, P.; Sihag, P.; Chaturvedi, P.; Uday, K.; Dutt, V. BS-LSTM: An ensemble recurrent approach to forecasting soil movements in the real world. *Front. Earth. Sci.* **2021**, *9*, 696792. [CrossRef]
30. Li, B.; Li, R.; Sun, T.; Gong, A.; Tian, F.; Khan, M.; Ni, G. Improving LSTM hydrological modeling with spatiotemporal deep learning and multi-task learning: A case study of three mountainous areas on the Tibetan Plateau. *J. Hydro.* **2023**, *620*, 129401. [CrossRef]

31. Wang, H.; Xu, Y.; Tang, S.; Wu, L.; Cao, W.; Huang, X. Well log prediction while drilling using seismic impedance with an improved LSTM artificial neural networks. *Front. Earth Sci.* **2023**, *11*, 1153619. [CrossRef]
32. Chen, K.; Zhou, Y.; Dai, F. A LSTM-based method for stock returns prediction: A case study of China stock market. In Proceedings of the 2015 IEEE International Conference on Big Data, Santa Clara, CA, USA, 29 October–1 November 2015.
33. Chen, S.; Ge, L. Exploring the attention mechanism in LSTM-based Hong Kong stock price movement prediction. *Qua. Financ.* **2019**, *19*, 1507–1515. [CrossRef]
34. Liu, S.; Zhang, C.; Ma, J. CNN-LSTM neural network model for quantitative strategy analysis in stock markets. In Proceedings of the Neural Information Processing, Guangzhou, China, 14–18 November 2017.
35. Zhang, L.; Wu, X.; Ji, W.; AbouRizk, S.M. Intelligent approach to estimation of tunnel-induced ground settlement using wavelet packet and support vector machines. *J. Comput. Civ. Eng.* **2017**, *31*, 04016053. [CrossRef]
36. Kim, T.; Cho, S. Predicting residential energy consumption using CNN-LSTM neural networks. *Energy* **2019**, *182*, 72–81. [CrossRef]
37. Iervolino, I. Asymptotic behavior of seismic hazard curves. *Struct. Saf.* **2022**, *99*, 102264. [CrossRef]
38. Lagomarsino, S.; Cattari, S.; Angiolilli, M.; Bracchi, S.; Rota, M.; Penna, A. Modelling and seismic response analysis of existing URM structures. Part 2: Archetypes of Italian historical buildings. *J. Earthq. Eng.* **2023**, *27*, 1849–1874. [CrossRef]
39. Aloisio, A.; De Santis, Y.; Irti, F.; Pasca, D.P.; Scimia, L.; Fragiacomo, M. Machine learning predictions of code-based seismic vulnerability for reinforced concrete and masonry buildings: Insights from a 300-building database. *Eng. Struct.* **2024**, *301*, 117295. [CrossRef]
40. Tang, L.; Na, S. Comparison of machine learning methods for ground settlement prediction with different tunneling datasets. *J. Rock Mech. Geotech. Eng.* **2021**, *13*, 1274–1289. [CrossRef]
41. Vu, N.M.; Nguyen, L.V.; Dao, L.P. Methods for mitigating effects induced by tunnelling on nearby existing buildings in cities. *J. Min. Earth Sci.* **2020**, *61*, 57–65. [CrossRef]
42. Mohammadi, S.D.; Naseri, F.; Alipoor, S. Development of artificial neural networks and multiple regression models for the NATM tunnelling-induced settlement in Niayesh subway tunnel. *Tehran. Bull. Eng. Geol. Environ.* **2015**, *74*, 827–843. [CrossRef]
43. Tan, Y.; Wang, D. Structural behaviors of large underground earth-retaining systems in Shanghai. II: Multipropped rectangular diaphragm wall. *J. Perform. Constr. Facil.* **2015**, *29*, 04014059. [CrossRef]
44. Hochreiter, S.; Schmidhuber, J. Long short-term memory. *Neural Comput.* **1997**, *9*, 1735–1780. [CrossRef] [PubMed]
45. Li, G.; Zhao, X.; Fan, C.; Fang, X.; Li, F.; Wu, Y. Assessment of long short-term memory and its modifications for enhanced short-term building energy predictions. *J. Build. Eng.* **2021**, *43*, 103182. [CrossRef]
46. Kandel, I.; Castelli, M. The effect of batch size on the generalizability of the convolutional neural networks on a histopathology dataset. *Ict Express* **2020**, *6*, 312–315. [CrossRef]
47. Darabi, A.; Ahangari, K.; Noorzad, A.; Arab, A. Subsidence estimation utilizing various approaches–A case study: Tehran No. 3 subway line. *Tunn. Undergr. Space Technol.* **2012**, *31*, 117–127. [CrossRef]